Available online at www.sciencedirect.com
ScienceDirect
Journal of Sound and Vibration 304 (2007) 345–360
JOURNAL OF SOUND AND VIBRATION
www.elsevier.com/locate/jsvi

An active damping control of robot manipulators with oscillatory bases by singular perturbation approach

J. Lin*, Z.Z. Huang, P.H. Huang

Department of Mechanical Engineering, Ching Yun University, 229, Chien-Hsin Road, Jung-Li City, Taiwan 320, ROC

Received 20 September 2006; received in revised form 6 December 2006; accepted 4 March 2007

Abstract

This paper deals with active damping control problems of robot manipulators with oscillatory bases. A first investigation of two-time scale fuzzy logic controller with vibration stabilizer for such structures has been proposed, where the dynamics of a robotic system is strongly affected by disturbances due to the base oscillation. Under the assumption of two-time scale, its stability and design procedures are presented for a multiple link manipulator with multiple dimension oscillation. The fast-subsystem controller will damp out the vibration of the oscillatory bases using a PD control method. Hence, the slow-subsystem fuzzy logic controller dominates the trajectory tracking. It can be guaranteed the stability of the internal dynamics by adding a boundary-layer correction based on singular perturbations approach. Experimental results have shown that the proposed control model offers several implementation advantages such as reduced effect of overshoot and chattering, smaller steady state error, and a fast convergent rate. The results of this study can be feasible to various mechanical systems, such as mobile robot, gantry cranes, underwater robot, and other dynamic systems mounted on oscillatory bases.

1. Introduction

The interest toward complex robot system is expanding for new application areas. An example of such a system is a dexterous manipulator mounted on an oscillatory base, which is, associated with robotic manipulators installed on vessels or ocean structures, where the dynamics of a robotic system is strongly affected by disturbances due to the base oscillation. In literature, such a system is known under the name macro–micro system or *flexible structure mounted manipulator system* (*FSMS*) [1].

Two main control subtasks for FSMS have been identified [2]: (1) base vibration suppression control and (2) design of control inputs that induce minimum vibrations. Most studies investigating oscillatory base manipulators falls examines inertial task space and external disturbances [3]. The primary issues of this kind of problem are manipulator decoupling, base dynamics and damping of base oscillation, for which several approaches, such as task-space feedback [4,5], filtering command [6], path planning [5], acceleration feedback [7], and active damping [8,9], have been proposed. Additionally, numerous studies have developed control

*Corresponding author. Tel.: +886 3 4581196x3300; fax: +886 3 4595684.
E-mail address: jlin@cyu.edu.tw (J. Lin).

0022-460X/$ - see front matter © 2007 Elsevier Ltd. All rights reserved.
doi:10.1016/j.jsv.2007.03.008

schemes for macro- and micro-manipulators [9,10]. One area of research involves determining trajectories that eliminate or minimize induced vibration [10]; however, such schemes are not useful for controlling the vibration once it occurs. An inertial damping scheme using a micromanipulator to dampen vibration is an attractive compromise between controlling system complexity and system performance [9,11]. However, all of the above papers never discussed the intelligent controller for such structures. Moreover, previous studies have several limitations, and have ignored many important issues, such as the interaction of the link and base oscillation, inertia uncertainties, and lack of availability of some states, among others.

Previous work by the authors [12] demonstrated the feasibility of the proposed control scheme using hierarchical supervisory fuzzy control. Generally, without the presence of additional sensors, strain gauges, and accelerometers, it is assumed that the displacement of the oscillatory base cannot be measured. Therefore, the controller is based on the lack of availability of the base oscillation states. Hence, the controller design of this literature [12] is founded on supervisory to deal with the subsystems interactions.

To maintain reasonable computational loading, a controller based on a reduced-order model has been proposed [13,14]. In recent years, singular perturbation theory has been shown to be a convenient strategy for 'reduced-order modeling'. It is well known that the dynamics of singularly perturbed systems can be approximated by the dynamics of the corresponding reduced-order and boundary-layer subsystems for sufficiently small values of the singular perturbation parameter. The aim is to simplify the software and hardware implementation of the control algorithms while improving their robustness.

Therefore, the paper concentrates on fuzzy logic using singular perturbation approach for robot manipulators mounted on oscillatory bases. The proposed control methodology is based on the measurement and feedback of the joint and base oscillatory states. It is different from the reference [12], which the oscillatory states are not available in that paper. This research is the extension of the previous work [12] and present a new controller by singular perturbation approach. The controller has two separate feedback loops for positioning and damping, and the damping control is independent of manipulator positioning control. Consequently, the proposed damping control methodology can be easily added to existing position controlled robot manipulators.

2. System configuration

In this section, a mathematical model of the manipulator is obtained from independently known dynamics. Fig. 1 presents the conceptual model of a manipulator mounted on an oscillatory base. The oscillatory dynamics of the base can be simplified as a lumped mass with a spring. The dynamic equation of the motion is

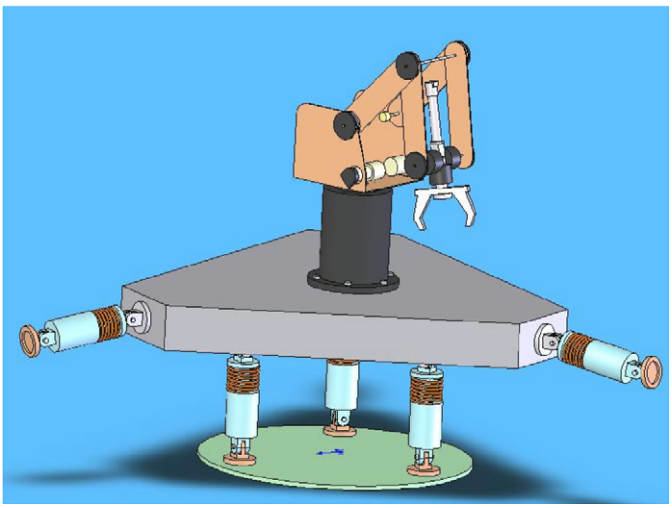

Fig. 1. Conceptual model of compliant manipulators.

represented as [8,12].

$$M_b\ddot{x}_b + C_b\dot{x}_b + K_b x_b = f_d, \tag{1}$$

where x_b denotes the deflection of the base from its equilibrium point. Moreover, M_b and K_b are the inertia matrix and stiffness matrix, respectively, and C_b is the damping matrix. In addition, the term of f_d is the excitation force acting on an oscillatory base.

Furthermore, the dynamics of the n rigid link manipulators with revolutional joints can be expressed as

$$M_r(q)\ddot{q} + V(q,\dot{q}) + F_v\dot{q} + F_d(\dot{q}) + G(q) = \tau \tag{2}$$

with $q(t) \in \Re^n$ as the joint variable vector and $\tau(t)$ as the control input. The inertial matrix $M_r(q)$ is assumed to be a bounded and positive definite matrix, where $V(q,\dot{q})$ is the Coriolis/centripetal forces, $F_v\dot{q}$ is viscous friction, $F_d(\dot{q})$ is dynamic friction, and $G(q)$ is gravity. It is assumed that $M_r(q)-2V$ is a skew-symmetrical matrix. Moreover, the dynamics of Eq. (2) may also be rewritten as

$$M_r(q)\ddot{q} + C_r(q,\dot{q}) = \tau \tag{3}$$

with nonlinear terms represented by

$$C_r(q,\dot{q}) = V(q,\dot{q}) + F_v\dot{q} + F_d(\dot{q}) + G(q).$$

When the two systems are serially combined, detailed analysis demonstrates that the overall system can be represented as

$$\begin{bmatrix} M_r(q) & M_{br}(X) \\ M_{br}^{\mathrm{T}}(X) & M_b + M_{b/r}(X) \end{bmatrix} \begin{Bmatrix} \ddot{q} \\ \ddot{x}_b \end{Bmatrix} + \begin{bmatrix} C_r(q,\dot{q}) + C_{b/r}(X,\dot{X}) \\ C_b\dot{x}_b + C_{br}(X,\dot{X}) \end{bmatrix} + \begin{bmatrix} 0 & 0 \\ 0 & K_b \end{bmatrix} \begin{Bmatrix} q \\ x_b \end{Bmatrix} = \begin{bmatrix} \tau \\ 0 \end{bmatrix}, \tag{4}$$

where $M_{b/r}(X)$ and $M_{br}(X)$ denote the inertia matrices for manipulator/base coupling, which can be referred to as the inertial coupling matrix. Additionally, both $C_{b/r}(X,\dot{X})$ and $C_{br}(X,\dot{X})$ are nonlinear coupling terms, and $X = [q^{\mathrm{T}} \; x_b^{\mathrm{T}}]^{\mathrm{T}}$. The inertia matrix of the overall system $\mathbf{M}(X)$ shown in Eq. (4) is symmetric and positive definite.

Moreover, the inertia matrix $\mathbf{M}(X)$ that is uniformly bounded both from above and from below, namely, satisfies

$$\underline{m} I_{n+p} \leqslant \mathbf{M}(X) \leqslant \bar{m} I_{n+p}, \quad \forall X \in \Re^{n+p},$$

where $\underline{m}$ and $\bar{m}$ are positive constants, and $I_{n+p} \in \Re^{(n+p)\times(n+p)}$ is the identity matrix. Here, p is defined as the number of degrees of freedom (dof) of the oscillatory base.

For practical applications, one mode (which is coupled with translation and rotation) is frequently dominant in structural oscillation. Controlling translation implies that rotation is also controlled. Therefore, this study focuses on translate oscillation as an initial study only. The assumption is the same as that in literature [8]. For exposition convenience, this work considers a special case, a two-link planar elbow arm mounted on an oscillatory base (Fig. 2), with a two dof manipulator and one-dof base motions.

In addition, the more description on the modeling process is shown in Appendix A.

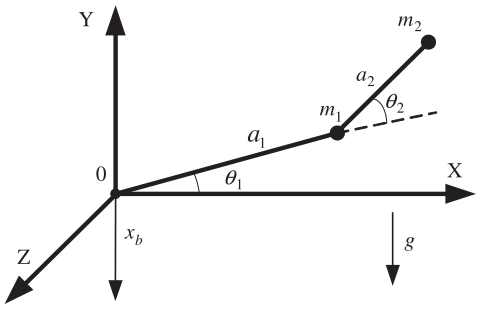

Fig. 2. Schematic view of the manipulator mounted on an oscillatory base.

3. Singular perturbation approach

In using input/output (I/O) feedback linearization to design a controller for flexible link arm is shown in the author previous work [13]. In this section, we will use the same technique to derive a singular perturbation formulation for a multiple link manipulator with multiple dimension oscillatory under two-time scale assumption. We will complete the design in Section 4 by using singular perturbation approach theory to design a controller that provides a boundary-layer correction to stabilize the oscillatory modes.

3.1. Inverse system dynamics

Let us define the inverse of the mass matrix

$$\begin{bmatrix} H_{11} & H_{12} \\ H_{21} & H_{22} \end{bmatrix} = \begin{bmatrix} M_r & M_{rb} \\ M_{rb}^{\mathrm{T}} & M_b + M_{b/r} \end{bmatrix}^{-1}. \tag{5}$$

We multiply (4) by (5) from the left, rearrange terms, and write

$$\begin{bmatrix} \ddot{q} \\ \ddot{x}_b \end{bmatrix} = -\begin{bmatrix} H_{11} & H_{12} \\ H_{21} & H_{22} \end{bmatrix} \begin{bmatrix} C_r(q,\dot{q}) + C_{b/r}(X,\dot{X}) \\ C_b\dot{x}_b + C_{br}(X,\dot{X}) \end{bmatrix} - \begin{bmatrix} H_{11} & H_{12} \\ H_{21} & H_{22} \end{bmatrix} \begin{bmatrix} 0 & 0 \\ 0 & K_b \end{bmatrix} \begin{bmatrix} q \\ x_b \end{bmatrix} + \begin{bmatrix} H_{11} & H_{12} \\ H_{21} & H_{22} \end{bmatrix} \begin{bmatrix} \tau \\ 0 \end{bmatrix}. \tag{6}$$

Therefore, Eq. (6) can be rewrite as the following form:

$$\ddot{q} = -H_{11}(C_r(q,\dot{q}) + C_{b/r}(X,\dot{X})) - H_{12}(C_b\dot{x}_b + C_{br}(X,\dot{X})) - H_{12}K_bx_b + H_{11}\tau, \tag{7}$$

$$\ddot{x}_b = -H_{21}(C_r(q,\dot{q}) + C_{b/r}(X,\dot{X})) - H_{22}(C_b\dot{x}_b + C_{br}(X,\dot{X})) - H_{22}K_bx_b + H_{21}\tau. \tag{8}$$

Performing a feedback linearization on (7) amounts to select

$$\tau = (H_{11})^{-1}(H_{11}(C_r(q,\dot{q}) + C_{b/r}(X,\dot{X})) + H_{12}(C_b\dot{x}_b + C_{br}(X,\dot{X})) + H_{12}K_bx_b + u). \tag{9}$$

Using standard I/O feedback linearization technique, then substitute for $\ddot{q}$ using (7), to obtain the reduced-order dynamics

$$\ddot{q} = u, \tag{10}$$

$$\begin{aligned} \ddot{x}_b = & -H_{21}(C_r(q,\dot{q}) + C_{b/r}(X,\dot{X})) - H_{22}(C_b\dot{x}_b + C_{br}(X,\dot{X})) - H_{22}K_bx_b \\ & + H_{21}(H_{11})^{-1}(H_{11}(C_r(q,\dot{q}) + C_{b/r}(X,\dot{X})) + H_{12}(C_b\dot{x}_b + C_{br}(X,\dot{X})) + H_{12}K_bx_b + u) \\ = & -(H_{22} - H_{21}(H_{11})^{-1}H_{12})C_b\dot{x}_b - (H_{22} - H_{21}(H_{11})^{-1}H_{12})C_{br}(X,\dot{X}) \\ & -(H_{22} - H_{21}(H_{11})^{-1}H_{12})K_bx_b + H_{21}(H_{11})^{-1}u. \end{aligned} \tag{11}$$

Eq. (11) can be rewrite as

$$\ddot{x}_b = -H_{22}^a C_b\dot{x}_b - H_{22}^a C_{br}(X,\dot{X}) - H_{22}^a K_bx_b + H^a u, \tag{12}$$

where $u(t)$ is an auxiliary input and the Schur complements are defined as

$$H_{22}^a = H_{22} - H_{21}(H_{11})^{-1}H_{12},$$
$$H^a = H_{21}(H_{11})^{-1}.$$

As shown in the first row of (6), the manipulator rigid motion is mostly decoupled from the base oscillation. The base motion has no effect on the joint motion. They are coupled only through the control input u. Moreover, the given joint trajectory $q_d(t)$ in Eq. (10) can be achieved by appropriate selection of u. However, selecting based only on the desired joint angle subsystem performance does not guarantee a stable inverse system as the zero dynamics are not stable for such system. Hence, we will show how to select $u(t)$ to achieve the desired joint angle performance as well as to stabilize the inverse dynamics using a time-scale separation in the next subsection.

3.2. A singular perturbation approach

We now use singular perturbation theory to stabilize the zero dynamics after input/output feedback linearization. As will be seen, this affords greater accuracy of the time-scale separation assumption. A typical procedure for singular perturbation theory is reviewed in Ref. [15].

The control scheme takes advantages of the fact that base vibration is of relatively high frequency compared to the rigid manipulator motion required to perform a task. The separation of bandwidths, or time constants, between the position and vibration control loops allows then to be considered separately. Therefore, we use the singular perturbation approach to derive a slow subsystem corresponding to the joint angle, and a fast subsystem describing the oscillatory base motion in this section. To singularly perturb the feedback-linearized system, we rewrite (10) and (11) as

$$\ddot{q} = u, \tag{13}$$

$$\ddot{x}_b + H_{22}^{a/b}\dot{x}_b + H_{22}^{a/br}(X, \dot{X}) + H_{22}^{a/Kb}x_b = H^a u, \tag{14}$$

where

$$H_{22}^{a/b} = H_{22}^{a}C_b,$$
$$H_{22}^{a/br} = H_{22}^{a}C_{br},$$
$$H_{22}^{a/Kb} = H_{22}^{a}K_b.$$

For the singular perturbation analysis to work, we must put (13) and (14) in the standard form and solve for fast variables. Since the oscillatory state is faster than the joint angle, we must extract an appropriate parameter from the fast subsystem first. We define

$$K^{\mathrm{cl}} = H_{22}^{a/Kb}, \tag{15}$$

where K^{cl} indicates the closed-loop stiffness and K_b is the open-loop stiffness appearing in Eq. (4). It is more accurate to introduce singular perturbation based on K^{cl} rather than on K_b. Therefore, we introduce a positive scaling factor κ and factor K^{cl} as

$$K^{\mathrm{cl}} = \kappa\tilde{K}^{\mathrm{cl}}, \tag{16}$$

where $\tilde{K}^{\mathrm{cl}}$ is an invertible constant matrix and is independent of the closed-loop stiffness factor κ.

Then define new variables $\varepsilon^2 = (1/\kappa)$ and $\varepsilon^2\xi(t) = x_b(t)$. We are concerned with the case where the stiffness κ is sufficiently large, and the main objective of our control is to let the rigid motion $q_r(t)$ track a desired trajectory $q(t)$.

Here, rewriting (13) and (14) in terms of $\xi(t)$, and ε we have

$$\ddot{q} = u, \tag{17}$$

$$\varepsilon^2\ddot{\xi} = -H_{22}^{a/b}(q, \dot{q}, \varepsilon^2\xi, \varepsilon^2\dot{\xi})\varepsilon^2\dot{\xi} - H_{22}^{a/br}(q, \dot{q}, \varepsilon^2\xi, \varepsilon^2\dot{\xi}) - \tilde{K}^{\mathrm{cl}}(q, \varepsilon^2\xi)\xi + H^a(q, \varepsilon^2\xi)u. \tag{18}$$

Recall that the control objective is to determine the control input u to let $(q, \dot{q})$ track $(q_d, \dot{q}_d)$ sufficiently closely and to stabilize systems (17) and (18). Therefore, a composite (fast and slow) controller is designed based on the partially decoupled model in Eqs. (17) and (18). Define the control input u to have two parts

$$u = \bar{u}(q) + u_f(x_b), \tag{19}$$

where $\bar{u}(q)$ is the slow control component and $u_f(x_b)$ is a fast control component. Setting $\varepsilon = 0$ yields the slow dynamics

$$\ddot{\bar{q}} = \bar{u} \tag{20}$$

and

$$0 = -\bar{H}_{22}^{a/br} - \bar{\tilde{K}}^{\mathrm{cl}}\bar{\xi} + \bar{H}^a\bar{u}. \tag{21}$$

Therefore, the slow manifold equation can solved from Eq. (21)

$$\bar{\xi} = (\bar{\tilde{K}}^{\mathrm{cl}})^{-1}(-\bar{H}_{22}^{a/br} + \bar{H}^{a}\bar{u}). \tag{22}$$

We use the overbar to denote evaluation of functions with $\varepsilon = 0$. Furthermore, to derive the fast subsystem, select new states $\varsigma_1 \equiv \xi - \bar{\xi}$, $\varsigma_2 \equiv \varepsilon\dot{\xi}$, and write (18) as

$$\varepsilon\dot{\varsigma}_2 = -H_{22}^{a/b}\varepsilon\varsigma_2 - H_{22}^{a/br} - \tilde{K}^{\mathrm{cl}}(\varsigma_1 + \bar{\xi}) + H^{a}u. \tag{23}$$

Moreover, we introduce a time-scale change of $\sigma = t/\varepsilon$. Setting $\varepsilon = 0$ and substituting for $\bar{\xi}$ from Eq. (22), the expression of fast subsystem can now be obtained by combining (22) and (23):

$$\frac{\mathrm{d}\varsigma_1}{\mathrm{d}\sigma} = \varsigma_2, \tag{24}$$

$$\frac{\mathrm{d}\varsigma_2}{\mathrm{d}\sigma} = -\bar{\tilde{K}}^{\mathrm{cl}}\varsigma_1 + \bar{H}^{a}u_f. \tag{25}$$

The state-space representation of the dynamics is

$$\frac{\mathrm{d}}{\mathrm{d}\sigma}\begin{bmatrix}\varsigma_1\\ \varsigma_2\end{bmatrix} = \begin{bmatrix}0 & 1\\ -\bar{\tilde{K}}^{\mathrm{cl}} & 0\end{bmatrix}\begin{bmatrix}\varsigma_1\\ \varsigma_2\end{bmatrix} + \begin{bmatrix}0\\ \bar{H}^{a}\end{bmatrix}u_f. \tag{26}$$

4. Controller design

The control objective attempts to determine the input control torque τ, such that base oscillation x_b damps out as efficiently as possible while the joint angle q follows the desired tracking. Using two-time scale theory, $\bar{u}$ and u_f are adopted in two different time scales. It is intended that u_f affects mainly on (25), base motion and $\bar{u}$ principally on (20), decoupled joint angle dynamics. In accordance with (20), (24) and (25), u_f can be chosen to generate stable zero dynamics provided that $(\bar{\tilde{K}}^{\mathrm{cl}}, \bar{H}^{a})$ can be stabilized. When $(\bar{\tilde{K}}^{\mathrm{cl}}, \bar{H}^{a})$ is controllable, there are no zero dynamics, as u_f can be chosen to control $[\varsigma_1^{\mathrm{T}}\ \varsigma_2^{\mathrm{T}}]^{\mathrm{T}}$. Consequently, the slow part, $\bar{\xi}$ in Eq. (22), depends on joint angle trajectories and the control, $\bar{u}$, was used to construct joint tracking controller. The fast part, ζ_1, is a boundary-layer correction added for stabilization.

4.1. Fuzzy tracking controller (FTC)

A primary goal in this subsection is to control actively trajectory tracking using a decomposed parallel fuzzy control approach. This study demonstrates the general methodology by decomposing a large-scale system into smaller subsystems in a parallel structure, such that the proposed fuzzy control methodology can be applied for investigating a complex system. A fuzzy logic controller is designed utilizing the joint tracking error between the desired and measured e ($e = \theta_d - \theta$) and the joint velocity error between the desired and measured $\dot{e}$ to implement an input–output feedback linearization/singular perturbation approach. To implement the proposed technique for a two-link robot manipulator, the whole system is decomposed into two subsystems. The first subsystem adopts joint tracking error e_1 ($e = \theta_d - \theta$) and its derivatives $\dot{e}_1$ as local variables for link 1 subsystem. The second subsystem takes e_2 and $\dot{e}_2$ as local variables for link 2 subsystem. Therefore, the fuzzy logic controller 1 (FLC1) takes e_1 and $\dot{e}_1$ as inputs to construct the local control action $\bar{u}_1$, whereas fuzzy logic controller 2 (FLC2) uses e_2 and $\dot{e}_2$ to take another control action, $\bar{u}_2$. Thus, at the local level, each subsystem is designed separately. The fuzzy logic rule base for each subsystem is designed based on the dynamic response for each link when a control force is activated on the robotic system.

This investigation uses the adaptive network-based fuzzy inference system (ANFIS) to optimize fuzzy IF-THEN rules and membership functions for deriving a more efficient fuzzy control. The main idea in the learning procedure is to update the membership function and fuzzy rule by using the information from the training patterns, i.e., sets of input–output outcomes. The training algorithm resembles that in Refs. [12,16].

It is worthy noted that, the adaptive-ANFIS handles smooth membership better than trapezoidal systems; bell-shaped functions are employed to convert these inputs and output variables into linguistic control variables. Usually, $\mu_{A_i}(x)$ is chosen to be bell shaped with a maximum equal to 1 and minimum equal to 0, such as

$$\mu_{A_i}(x : a, b, c) = \frac{1}{1 + |(x - c)/a|^{2b}}, \tag{27}$$

where $\{a, b, c\}$ is the parameter set. Additionally, in this study, linguistic variables corresponding to *large negative* (LN), *small negative* (SN), *zero* (ZE), *small positive* (SP), and *large positive* (LP) are used to represent domain knowledge [16].

Consequently, the first order of the Takagi-Sugeno-Kang (TSK) model ANFIS structure containing 25 rules was considered. The bell-shaped membership functions with product inference rules were utilized at the fuzzification level. The resulting vector is defuzzified by the first-order TSK model. To characterize the controller, an ANFIS network with the fuzzifier processing two inputs, the rule base containing 25 rules and

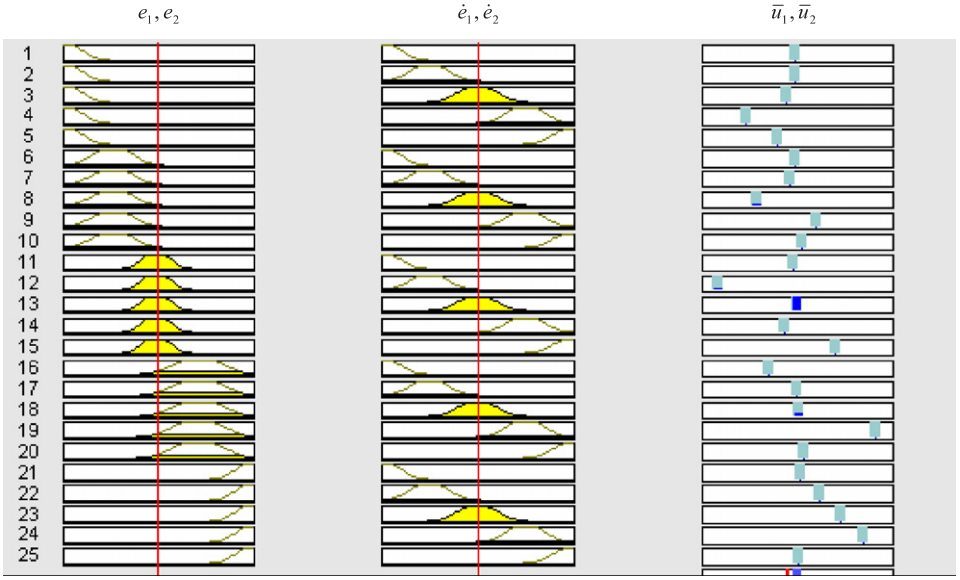

Fig. 3. Rule view for fuzzy tracking controller.

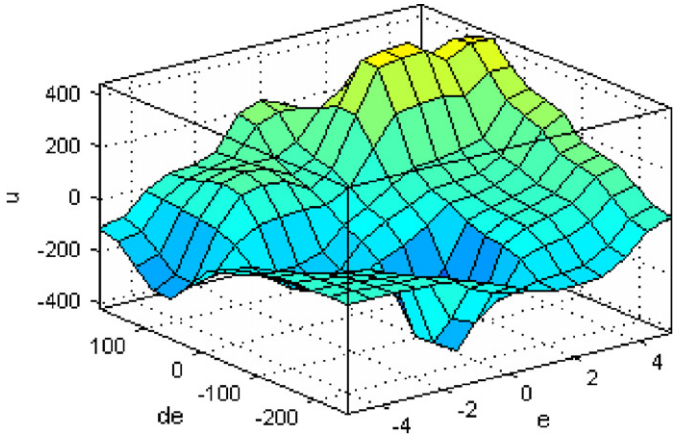

Fig. 4. Control surface view of the proposed fuzzy system.

the defuzzifier comprising one output was trained. Fig. 3 displays the rule view window for FTC. Fig. 4 presents the control surface view of the proposed fuzzy system. More detail discussion of the fuzzy controller and ANFIS procedure, please refer to the previous of the authors work [12,16].

4.2. Boundary-layer stabilizer (active damping controller)

The boundary-layer stabilizer (or active damping controller), u_f, is selected to stabilize the fast subsystem (26). Since the fast subsystem is only a linearization of oscillatory dynamics induced by the slow manifold $\bar{\xi}$, the fast control law is used to stabilize the inverse system dynamics. Therefore, u_f can be designed as a PD control for the boundary layer. Therefore, we propose the control law

$$u_f = -\mathbf{K}\varsigma, \quad \varsigma = [\varsigma_1 \ \ \varsigma_2]^{\mathrm{T}}. \tag{28}$$

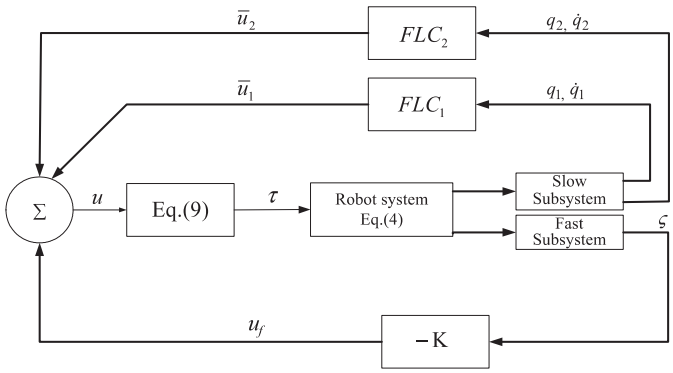

Fig. 5. Block diagram of the hybrid system.

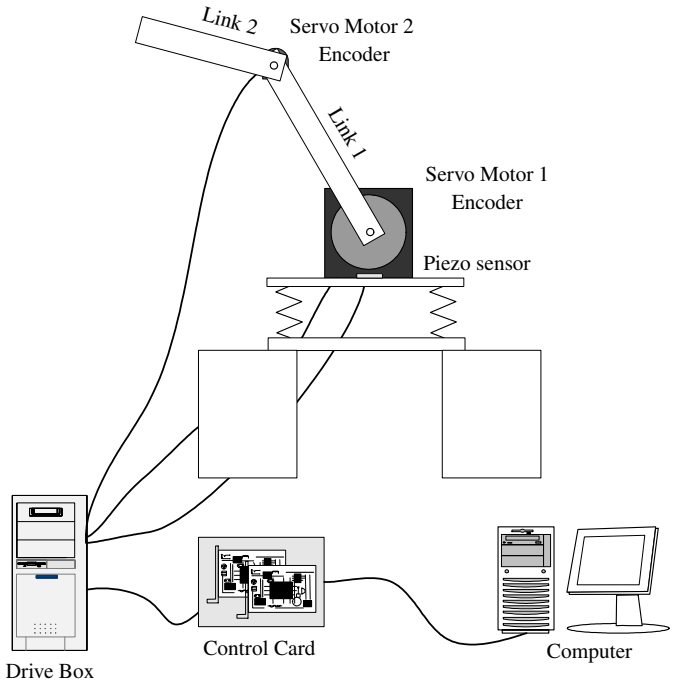

Fig. 6. Schematic diagram of control experiment.

With a proper (positive) **K**, a damped vibration system is obtained, and, hence, vibration suppression will be guaranteed. The damping of the base oscillation can be adjusted by modifying the control gain **K**. The composite control scheme is adopted. By combining the slow control component $\bar{u}$ and fast control

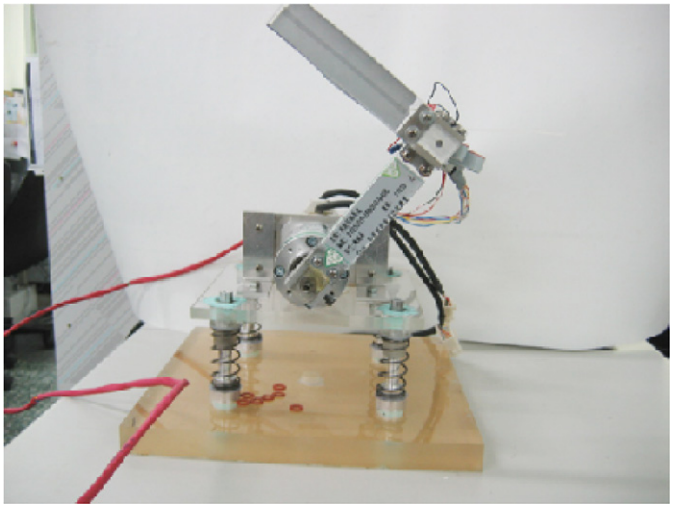

Fig. 7. Overview of experimental system.

Table 1
System parameters

Parameter	Value	Parameter	Value
m_2	0.3872 kg	m_2	0.1194 kg
a_2	0.155 m	a_2	0.145 m
M_b	3.027 kg	K_b	800 N/m

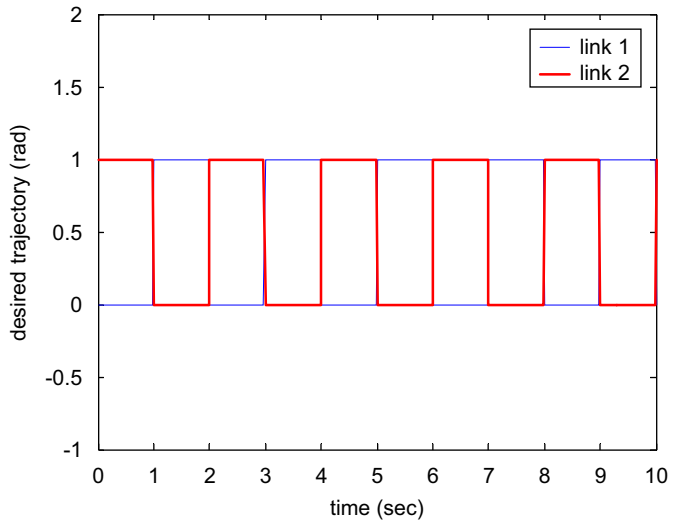

Fig. 8. Desired joint step pulse trajectory for links 1 and 2.

component u_f, the system follows the desired joint trajectory and suppresses base vibration. Fig. 5 presents a block diagram of the hybrid system.

5. Experimental implementation

The test bed at Ching Yun University consists of a two-link rigid manipulator mounted on an oscillatory base (Fig. 6). Fig. 7 shows an overview of experimental system. Two servomotors (provided by Panasonic and Maxon) are attached to each joint with optical encoders for measuring the position of the motor shaft. Optical encoders are used as position feedback devices for sensing the angular displacement of the motor shaft. Moreover, base compliance was achieved with four linear springs (stiffness 200 N/m for each spring). Base vibration is measured using a PCB PIEZOTRONICS Model 208C01 force sensor, which is attached on the oscillatory base face. The input torque to the manipulator system is derived by the computer based on the joint and base displacements, and is sent through a digital/analog (D/A) board to amplifiers driving current to the motors in the joints. Test results are acquired using the aforementioned procedures, MATLAB and Simulink. Table 1 lists system parameters. As each link moved, the base oscillated due to compliance. Since the manipulator is attached at a pivot joint, its base exhibits translation and rotation as each link moves.

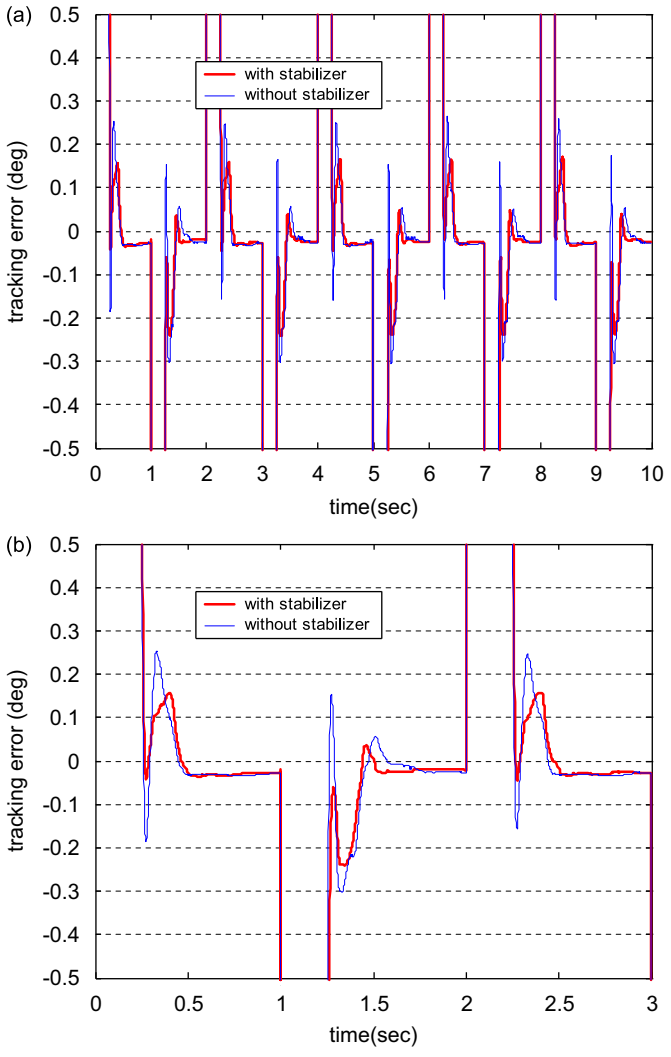

Fig. 9. Experimental results for tracking error under step pulse trajectory (link 1).

However, these two motions are not independent. Thus, controlling translational oscillation implies controlling rotational motion at the same time in this case. Therefore, for feedback controller design, only base translation is considered in this experiment.

6. Results and discussions

This section presents overall experimental results for the proposed controller for such a robotic system. To verify the controller's performance, some step pulse input real-time experiments carried out for the proposed control scheme are described. The desired step input was taken as one radian amplitude and 1 period second for link 1 and 2, respectively (Fig. 8). The calculation for controlling results is according to procedures in Sections 3 and 4.

Figs. 9 and 10 present the joint angle errors with fuzzy tracking control and a boundary-layer stabilizer (damping controller) for link 1 and link 2, respectively. A pure FTC can achieve good transient tracking performance (Fig. 9) for link 1 tracking control. Fig. 9(b) denotes the fine scale for tracking performance at 0–3 s. However, Fig. 9 indicates that pure FTC causes a large overshoot during the transition. In such a case, the control system is subjected to severe chattering due the base oscillation. To reduce the overshoot, the boundary-layer stabilizer was applied. This experimental finding demonstrates that performance was

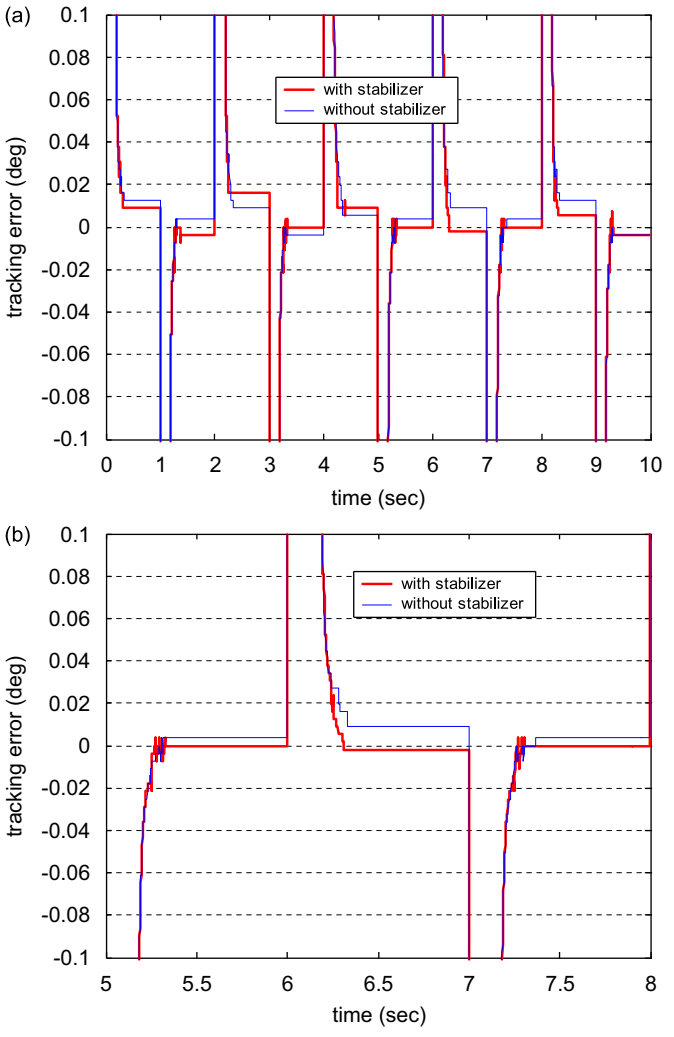

Fig. 10. Experimental results for tracking error under step pulse trajectory (link 2).

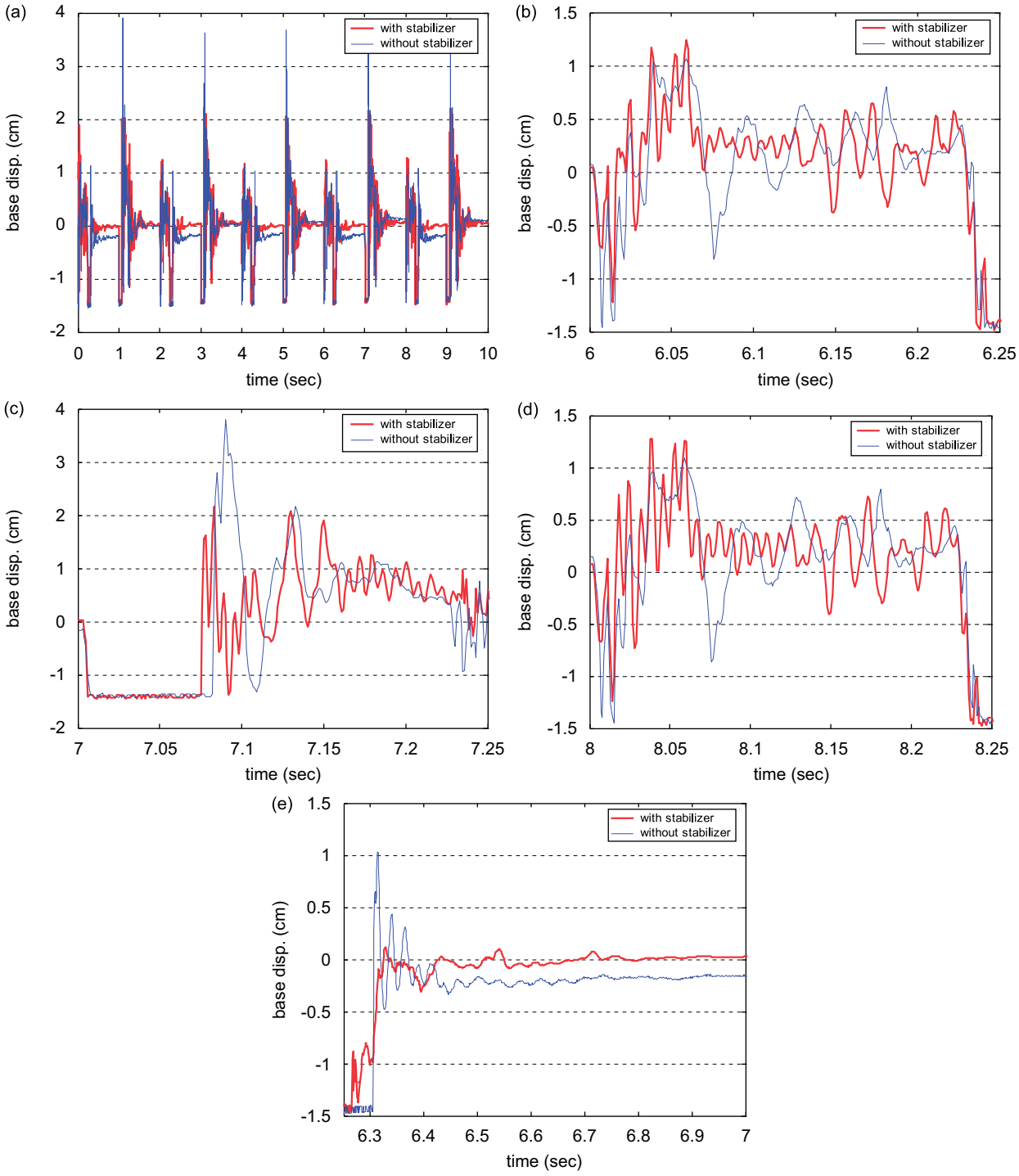

Fig. 11. Experimental results of the oscillatory base vibration displacement x_b of with and without damping control: (a) transient response during [0, 10] s; (b) transient response during [6, 6.25] s; (c) transient response during [7, 7.25] s; (d) transient response during [8, 8.25] s; (e) transient response during [6.25, 7] s.

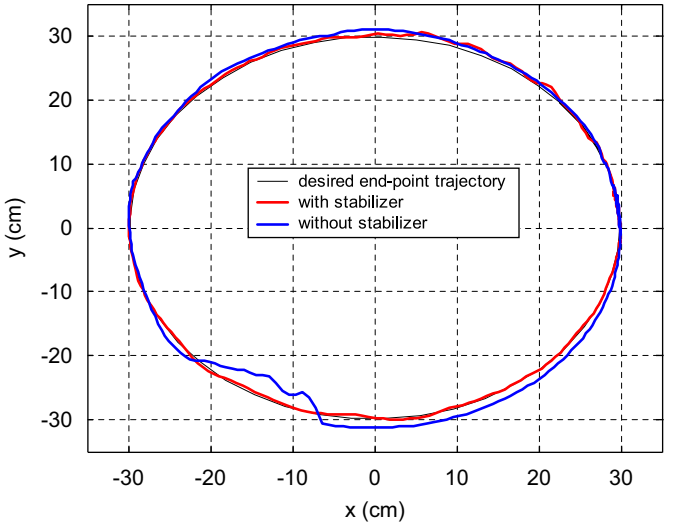

Fig. 12. Tip position for circular desired path.

improved markedly for joint angle θ_1 when the boundary-layer stabilizer was applied (Fig. 9). The maximum overshoot was reduced considerably.

Fig. 10 displays the tracking response for joint angle θ_2. There was a little improvement in the joint tracking when the boundary-layer stabilizer was applied. The steady-state error was reduced from $1.3e{-}2$ (without the boundary-layer stabilizer) to $5.4e{-}3$ (with the boundary-layer stabilizer) from 5 to 8 s (Fig. 10(b)). This experimental finding proves that the active damping controller reduces joint angle steady-state tracking error owing to uncontrolled vibration by approximately 58.5%. These experimental results demonstrate that the proposed control system achieves excellent tracking performance and satisfactorily attenuates disturbances due to base oscillation.

Base vibration was measured from the PCB PIEZOTRONICS Model 208C01 force sensor. Fig. 11 presents experimental results for base vibration with and without the boundary-layer stabilizer. The effectiveness of vibration suppression was confirmed when the boundary-layer stabilizer was applied. Figs. 11(b)–(d) presents the transient responses during [6, 6.25], [7, 7.25], and [8, 8.25] s. The maximum overshoot was clearly reduced once the boundary-layer stabilizer was introduced. Additionally, the steady-state base oscillation displacement was reduced from $1.5e{-}1$ (without the boundary-layer stabilizer) to $3.1e{-}2$ (with the boundary-layer stabilizer) from 6.25 to 7 s, a reduction vibration of 79.8% in settling time (Fig. 11(e)). Moreover, the normalized root-mean-square (rms) base oscillation sensor output voltage was reduced from 0.632 to 0.382, revealing that the proposed active damping controller reduces displacement due to uncontrolled vibration by roughly 40%. These experimental results verify the effectiveness of the proposed control methodology for minimizing base oscillatory vibration in the time domain. The active damping control action considerably diminishes the overshoot, and significantly reduces the steady-state error in settling time, demonstrating that the convergence rate is faster with than without the boundary layer stabilizer.

Next, a circular motion with a radius of 30 cm was given as an end-point desired trajectory with 3 s of travel time. The desired step input was taken as 2π radian amplitude and 1 period second for link 1, and 0 amplitude for link 2, respectively. Therefore, for the two-link revolute joint robotic arm, the tip of the arm link can be assumed to track the circle of the radius 30 cm. The desired joint motions (Fig. 12) show the tip position response for the circular motion. The solid line (black) is the desired endpoint trajectory. The dashed line (red) is the tracking performance with the boundary-layer stabilizer, and the dash–dotted line (blue) represents the tracking performance without the boundary-layer stabilizer. Comparing experimental results, the red line drew a more perfect circle as it did not oscillate as much as the blue line. The normalized rms tracking error was also reduced from 0.447 to 0.155, approximately a 65.3% reduction. These experimental results indicate that effective tracking performance was achieved and base oscillation can be eliminated. We conclude that the

controller was effective while the boundary-layer stabilizer. Consequently, the proposed control scheme addresses joint tracking performance, and enhances Cartesian endpoint accuracy.

7. Conclusions

An active damping controller for a manipulator mounted on an oscillatory base is proposed in this paper. A first investigation of two-time scale fuzzy logic controller plus stabilizer for such structures has been proposed, where the dynamics of a robotic system is strongly affected by disturbances due to the base oscillation. The fast-subsystem controller will damp out the vibration of the oscillatory bases using a PD control method. Hence, the slow-subsystem fuzzy logic controller dominates the trajectory tracking. It can be guaranteed that the stability of the internal dynamics by adding a boundary-layer correction based on singular perturbations approach. The proposed active damping control action considerably diminish the overshoots, significantly reduces the steady-state error in settling time, demonstrating that the convergence rate is faster than without the boundary-layer stabilizer. Consequently, the control design method proposed for this structure is found to be promising. The results of this study can be feasible to various mechanical systems, such as mobile robot, gantry cranes, underwater robot, and other dynamic systems mounted on oscillatory bases.

Acknowledgments

The authors would like to thank the National Science Council of the Republic of China, Taiwan for financially supporting this research under Contract No. NSC 94-2213-E-231-010.

Research Supported by National Science Council Research Grant NSC 94-2213-E-231-010.

Appendix A

As seen from Fig. 2, the position vector of links 1 and 2 can be shown as the below:

$$x_1 = a_1 \cos\theta_1, \qquad y_1 = a_1 \sin\theta_1 + x_b,$$
$$x_2 = a_1 \cos\theta_1 + a_2 \cos(\theta_1 + \theta_2), \qquad y_2 = a_1 \sin\theta_1 + a_2 \sin(\theta_1 + \theta_2) + x_b.$$

The velocity vector for each link is

$$\dot{x}_1 = -a_1\dot{\theta}_1 \sin\theta_1, \qquad \dot{y}_1 = a_1\dot{\theta}_1 \cos\theta_1 + \dot{x}_b,$$
$$\dot{x}_2 = -a_1\dot{\theta}_1 \sin\theta_1 - a_2(\dot{\theta}_1 + \dot{\theta}_2)\sin(\theta_1 + \theta_2), \qquad \dot{y}_2 = a_1\dot{\theta}_1 \cos\theta_1 + a_2(\dot{\theta}_1 + \dot{\theta}_2)\cos(\theta_1 + \theta_2) + \dot{x}_b.$$

The kinetic energy for the oscillatory bases $K_b = \frac{1}{2}M_b\dot{x}_b^2$

The kinetic energy for link 1

$$K_1 = \tfrac{1}{2}m_1(\dot{x}_1^2 + \dot{y}_1^2) = \tfrac{1}{2}m_1(a_1^2\dot{\theta}_1^2 + \dot{x}_b^2 + 2a_1\theta_1\dot{x}_b \cos\theta_1).$$

The kinetic energy for link 2

$$K_2 = \tfrac{1}{2}m_2(\dot{x}_2^2 + \dot{y}_2^2) = \tfrac{1}{2}m_2[a_1^2\dot{\theta}_1^2 + a_2^2(\dot{\theta}_1 + \dot{\theta}_2)^2 + 2a_1a_2(\dot{\theta}_1^2 + \dot{\theta}_1\dot{\theta}_2)\cos\theta_2 + 2a_1\dot{\theta}_1\dot{x}_b \cos\theta_1 + 2a_2\dot{x}_b(\dot{\theta}_1 + \dot{\theta}_2)\cos(\theta_1 + \theta_2) + \dot{x}_b^2].$$

The potential energy for the oscillatory bases $P_b = \frac{1}{2}K_bx_b^2$

The potential energy for link 1 $P_1 = mgy_1 = m_1g(a_1 \sin\theta_1 + x_b)$.

The potential energy for link 2 $P_2 = m_2gy_2 = m_2g[a_1 \sin\theta_1 + a_2 \sin(\theta_1 + \theta_2) + x_b]$.

The equations of motion are derived using Lagrangian formulation

$$\frac{\mathrm{d}}{\mathrm{d}t}\frac{\mathrm{d}L}{\mathrm{d}\dot{X}} - \frac{\mathrm{d}L}{\mathrm{d}X} = \tau, \qquad (5)'$$

where the Lagrangian $L = (K_1 + K_2 + K_b) - (P_1 + P_2 + P_b)$ is the difference between the kinetic and potential energies, $X = [q^T \ x_b^T]^T$.

Consequently, the overall dynamics equation of a two-link planar elbow arm mounted on an oscillatory base is the same as that in Eq. (4), where the joint variable is $= [\theta_1 \ \theta_2]^T$, and generalized force vector is $\tau = [u_1 \ u_2]^T$ with u_1 and u_2 torques supplied by actuators.

Additionally, the symbolic terms in Eq. (4) are

$$M_r = \begin{bmatrix} (m_1+m_2)a_1^2 + m_2a_2^2 + 2m_2a_1a_2\cos\theta_2 & m_2a_2^2 + m_2a_1a_2\cos\theta_2 \\ m_2a_2^2 + m_2a_1a_2\cos\theta_2 & m_2a_2^2 \end{bmatrix},$$

$$M_{b/r} = m_1 + m_2,$$

$$M_{br}^T = \begin{bmatrix} (m_1+m_2)a_1\cos\theta_1 + m_2a_2\cos(\theta_1+\theta_2) & m_2a_2\cos(\theta_1+\theta_2) \end{bmatrix},$$

$$C_{br} = -(m_1+m_2)a_1\dot{\theta}_1^2\sin\theta_1 - m_2a_2(\dot{\theta}_1+\dot{\theta}_2)^2\sin(\theta_1+\theta_2) + (m_1+m_2)gx_b,$$

$$C_r = \begin{bmatrix} -m_2a_1a_2(2\dot{\theta}_1\dot{\theta}_2 + \dot{\theta}_2^2)\sin\theta_2 + (m_1+m_2)ga_1\cos\theta_1 + m_2ga_2\cos(\theta_1+\theta_2) \\ m_2a_1a_2\dot{\theta}_1^2\sin\theta_2 + m_2ga_2\cos(\theta_1+\theta_2) \end{bmatrix},$$

$$C_{b/r} = \begin{bmatrix} -(m_1+m_2)a_1\dot{x}_b\dot{\theta}_1\sin\theta_1 \\ 0 \end{bmatrix},$$

where we assume that the link masses m_1 and m_2 are concentrated at the ends of the link, and a_1 and a_2 are link lengths, respectively [12].

Consequently, manipulator dynamics are strongly impacted by nonlinear forces due to base oscillation and its nonlinearity; these include gravity, Coriolis, and centrifugal forces, which are typically intrinsic to a mechanical system.

References

[1] A. Sharon, D. Hardt, Enhancement of robot accuracy using end-point feedback and a macro–micro manipulator system, *Proceedings of the 1984 American Control Conference*, San Diego, 1984, pp. 1836–1842.

[2] D.W. Cannon, D.P. Magee, W.J. Book, Experimental study on micro/macro manipulator vibration control, *Proceedings of the IEEE International Conference on Robotics and Automation*, Minneapolis, MN, 1996, pp. 2549–2554.

[3] M. Toda, Robust control for mechanical systems with oscillatory bases, *Proceedings of the IEEE Conference Systems, Man, and Cybernetics* 2 (1999) 878–893.

[4] D.N. Nenchev, K. Yoshida, M. Uchiyama, Reaction null-space based control of flexible structure mounted manipulator systems, *Proceedings of the 35th Conference on Decision and Control*, Kobe, Japan, 1996, pp. 4118–4123.

[5] D.N. Nenchev, K. Yoshida, P. Vichitkulsawat, A. Konno, M. Uchiyama, Experiments on reaction null-space based decouple control of a flexible structure mounted manipulator system, *Proceedings of the of IEEE Conference on Robotics and Automation*, Albuqerque, New Mexico, 1997, pp. 2528–2534.

[6] D.P. Magee, W.J. Book, Filtering micro-manipulator wrist commands to prevent flexible base motion, *Proceedings of the American Control Conference* (1995) 924–928.

[7] J.Y. Lew, S.-M. Moon, Acceleration feedback control of compliant base manipulators, *Proceedings of the 1999 American Control Conference*, San Diego, CA, 1999, pp. 1955–1959.

[8] J.Y. Lew, S.-M. Moon, A simple active damping control for compliant base manipulators, *IEEE/ASME Transactions on Mechatronics* 6 (3) (2001) 305–310.

[9] L.E. George, W.J. Book, Inertial vibration damping control of a flexible base manipulator, *IEEE/ASME Transactions on Mechatronics* 8 (2) (2003) 268–271.

[10] K. Yoshida, D. Nenchev, M. Uchiyama, Vibration suppression and zero reaction maneuvers of flexible space structure mounted manipulators, *Smart Materials and Structure* 8 (6) (1999) 847–856.

[11] W. Book, J. Loper, Inverse dynamics for commanding micromanipulator inertial forces to damp micromanipulator vibration, *Proceedings of the IEEE Robot Society of Japan International Conference On Intelligent Robots and Systems* 2 (1999) 707–714.

[12] J. Lin, A hierarchical supervisory fuzzy controller for robot manipulators with oscillatory bases, FUZZ-IEEE 2006, Vancouver, BC, Canada, July 16–21, 2006, pp. 10861–10868.

[13] J. Lin, F.L. Lewis, Two-time scale fuzzy logic controller of flexible link robot arm, *Fuzzy Sets and Systems* 139 (1) (2003) 125–149.

[14] J. Lin, Hierarchical fuzzy logic controller for a flexible link robot arm performing constrained motion tasks, *IEE Proceedings—Control Theory and Applications* 150 (4) (2003) 355–364.
[15] P.V. Kokotovic, H.K. Khalil, J. O'Reilly, *Singular Perturbation Methods in Control: Analysis and Design*, Academic Press, New York, 1986.
[16] J. Lin, A vibration absorber of smart structures using adaptive networks in hierarchical fuzzy control, *Journal of Sound and Vibration* 287 (4) (2005) 683–705.